BIOCHEMISTRY

 Volume 45, Number 22 June 6, 2006

Articles

Formation of a Complex of 5,10,15,20-Tetrakis(*N*-methylpyridinium-4-yl)-21*H*,23*H*-porphyrin with G-Quadruplex DNA†

Hajime Mita,‡ Takako Ohyama,‡ Yoshiyuki Tanaka,§ and Yasuhiko Yamamoto*,‡

Department of Chemistry, University of Tsukuba, Tsukuba 305-8571, Japan, and Laboratory of Molecular Transformation, Graduate School of Pharmaceutical Sciences, Tohoku University, Sendai, Miyagi 980-8578, Japan

Received November 30, 2005; Revised Manuscript Received March 23, 2006

ABSTRACT: A water-soluble cationic porphyrin, 5,10,15,20-tetrakis(*N*-methylpyridinium-4-yl)-21*H*,23*H*-porphyrin (TmPyP4), has been studied extensively because of its unique physicochemical properties that lead to interactions with nucleic acids, as well as its therapeutic application. Formation of a complex between TmPyP4 and parallel G-quadruplex DNA formed from a single repeat sequence of the human telomere, d(TTAGGG), has been characterized in an effort to elucidate the mode of molecular recognition between TmPyP4 and the DNA. The study demonstrated that TmPyP4 intercalates into the A3pG4 step of $[d(TTAGGG)]_4$ with an association constant of 6.2×10^6 M^{-1} and a stoichiometric ratio of 1:1. The binding of TmPyP4 to the A3pG4 step of $[d(TTAGGG)]_4$ was found to be stabilized by the $\pi-\pi$ stacking interaction of the porphyrin ring of TmPyP4 with the G4 quartet as well as the A3 bases of the G-quadruplex DNA. These findings provide novel insights for the design of porphyrin derivatives that bind to DNA with high affinity and specificity.

G-Quadruplex DNA is a four-stranded helix structure composed of stacked quartets known as G-quartets, each of which involves the planar association of four guanine bases in a cyclic Hoogsteen hydrogen bonding arrangement. At the terminus of a eukaryotic chromosome, a guanine-rich repeating sequence is found, which is thought to form a G-quadruplex (*1*−*5*). This sequence has received considerable interest in DNA-directed drug design (*6*−*10*).

The size and planarity of the porphyrin ring are well-suited for interaction with a G-quartet through $\pi-\pi$ stacking. 5,10,15,20-Tetrakis(*N*-methylpyridinium-4-yl)-21*H*,23*H*-porphyrin (TmPyP4,[1] structure shown in Figure 1) is a water-soluble cationic porphyrin and has been studied extensively because of its unique physicochemical properties that lead to interactions with nucleic acids, as well as its therapeutic application (*11*−*15*). TmPyP4 has been shown to bind to various nucleic acids such as duplex DNA (*16*−*22*) and RNA (*23*), DNA−RNA hybrids (*23*), triplex DNA (*24*, *25*), and quadruplex DNA (*26*−*30*). The way TmPyP4 binds to duplex DNA has been shown to depend greatly on the DNA

† This work was partly supported by a Grant-in-Aid (17655072) from MEXT, the Yazaki Memorial Foundation for Science and Technology, the NOVARTIS Foundation (Japan) for the Promotion of Science, and the University of Tsukuba, Research Project (A).

* To whom correspondence should be addressed. Phone and fax: +81-29-853-6521. E-mail: yamamoto@chem.tsukuba.ac.jp.

‡ University of Tsukuba.

§ Tohoku University.

[1] Abbreviations: TmPyP4, 5,10,15,20-tetrakis(*N*-methylpyridinium-4-yl)-21*H*,23*H*-porphyrin; K_a, association constant; CD, circular dichroism; T_m, melting temperature; NOE, nuclear Overhauser effect; NOESY, two-dimensional nuclear Overhauser effect spectroscopy; R_{TmPyP4}, $[TmPyP4]/[[d(TTAGGG)]_4]$, where [TmPyP4] and $[[d(TTAGGG)]_4]$ represent the concentrations of TmPyP4 and $[d(TTAGGG)]_4$, respectively; *n*, number of binding sites.

10.1021/bi052442z CCC: $33.50
Published on Web 05/13/2006

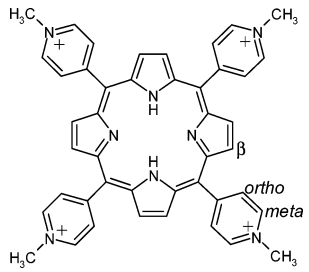

FIGURE 1: Molecular structure of 5,10,15,20-tetrakis(*N*-methylpyridinium-4-yl)-21*H*,23*H*-porphyrin (TmPyP4).

sequence and solution conditions. For example, TmPyP4 has been shown to intercalate between G-C base pairs (*20*, *31*, *32*) and also to bind to the major groove (*33*), minor groove (*17*, *34*), and surface of the DNA surface (*35*). The association constant (K_a) for binding of TmPyP4 to AT-rich sequences, through a major groove, has been reported to be comparable to that of the intercalation of TmPyP4 between G-C base pairs (*33*). A structural model of TmPyP4 binding preferentially to the major groove has been proposed on the basis of NMR structure characterization (*33*). Furthermore, in the cases of RNA duplex and the DNA−RNA hybrid, the binding of TmPyP4 has been shown to depend on base pairings and ribose puckering of target strands (*23*). TmPyP4 has also been shown to bind to triplex DNA, although the details of the complex formation are not fully understood. Recently, it has been shown that TmPyP4 interacts with G-quadruplex DNA and that the binding of TmPyP4 to the DNA inhibits telomerase activity (*30*). It has been proposed, on the basis of a molecular modeling study, that the stacking intercalation of TmPyP4 between adjacent G-quartet planes of G-quadruplex DNA stabilizes the complex (*30*). Thus, TmPyP4 is capable of binding to various sequences and structures of DNA in a variety of manners, the K_a values being 10^4-10^7 M^{-1} (*23*, *33*, *36*), which are within the affinity range, i.e., 10^4-10^{10} M^{-1}, reported for various DNA-interactive compounds (*37*−*39*).

We present herein the results of NMR, absorption, and circular dichroism (CD) studies on the interaction of TmPyP4 with all-parallel type G-quadruplex DNA formed from d(TTAGGG) (*40*), a single repeat sequence of the human telomere, exhibiting a melting temperature (T_m) of >50 °C. The study demonstrated that TmPyP4 intercalates into the A3pG4 step of the G-quadruplex DNA, $[d(TTAGGG)]_4$, with a K_a value of 6.2×10^6 M^{-1}. The binding of TmPyP4 to $[d(TTAGGG)]_4$ was found to be greatly stabilized by the stacking interaction between the π-system of the porphyrin moiety of TmPyP4 and the G-quartet plane formed by G4 guanine bases as well as the electrostatic attraction between pyridinium ions of TmPyP4 and phosphate ions of the DNA backbone. A model study suggested that the $\pi-\pi$ stacking interaction between the porphyrin moiety of TmPyP4 and A3 adenine bases also contributes to complex formation. The knowledge of this association is valuable in the design of the molecular architecture of a novel DNA enzyme formed from G-quadruplex DNA and a porphyrin derivative.

MATERIALS AND METHODS

Sample Preparation. d(TTAGGG) purified with a C-18 Sep-Pak cartridge was purchased from Tsukuba Oligo Service Co. (Tsukuba, Japan). The oligonucleotide was obtained by ethanol precipitation and then desalted with a Microcon YM-3 device (Millipore, Bedford, MA). The concentration of the oligonucleotide was determined spectrophotometrically using the absorption value at 260 nm ($\epsilon_{260} = 6.89 \times 10^4$ cm^{-1} M^{-1}). TmPyP4 tosylate was purchased from Dojin Kagaku, Co. Ltd. (Kumamoto, Japan), and converted to the chloride salt as follows. TmPyP4 tosylate was dissolved in distilled water, and then a potassium iodide solution was added to the resulting solution to precipitate the iodide salt of TmPyP4. The precipitated iodide salt of TmPyP4 was dissolved in 0.1 M HCl and then applied to an ion-exchange column (Dowex 1X2 Cl^- form resin; mesh size, 200−400; Dow Chemicals, Midland, MI) to replace the iodide ion with the chloride ion. The TmPyP4 concentration was determined using an extinction coefficient (ϵ_{424}) of 2.26×10^6 cm^{-1} M^{-1}. Potassium phosphate buffer (50 mM, pH 7.0) containing 300 mM KCl was used as the solvent throughout the optical measurements. For NMR measurements, the oligonucleotide concentration was 2 mM, as a quadruplex form, in 300 mM KCl and 50 mM potassium phosphate buffer (pH 7.0). The ^2H_2O content in the samples was either ∼10 or ∼100%.

Absorption and CD Spectroscopies. Absorption spectra were recorded on a Beckman DU640 spectrometer over the spectral range of 200−700 nm. CD spectra were recorded on a JASCO J-720W spectrometer over the spectral range of 240−500 nm. The concentrations of TmPyP4 for the absorption and CD measurements were 3.0 and 6.0 μM, respectively. The T_m values of 3 μM $[d(TTAGGG)]_4$ in the absence and presence of a stoichiometric amount of TmPyP4 were determined from the temperature dependence of the hyperchromic effect on the absorbance at 260 nm. The temperature for each measurement was increased over the range of 25−85 °C, with a heating rate of 0.5 °C/min.

NMR Measurement. ^{1}H NMR spectra were recorded on a Bruker AVANCE-500 or 600 spectrometer operating at a ^{1}H frequency of 500 or 600 MHz, respectively. One-dimensional ^{1}H NMR spectra were obtained with a 20 ppm spectral width, 32k data points, a 2 s relaxation delay, and 64 transients at 25 °C. Water suppression was achieved by the Watergate method (*41*, *42*). The signal:noise ratio of the spectra was improved by apodization, which introduced 0.3 Hz line broadening. Two-dimensional nuclear Overhauser effect (NOESY) spectra of a mixture for which R_{TmPyP4} $\{[TmPyP4]/[[d(TTAGGG)]_4]\} = 0.2$ {where [TmPyP4] and $[[d(TTAGGG)]_4]$ represent the concentrations of TmPyP4 and $d[TTAGGG)]_4$, respectively} were acquired by quadrature detection in the phase-sensitive mode with a States−TPPI method (*43*), with a 10 000 Hz spectral width, 4k × 1k data points, a 2 s relaxation delay, and a mixing time of 120, 200, or 300 ms at 25 °C. A phase-shifted sine-squared window function was applied to both dimensions before two-dimensional Fourier transformation. Chemical shifts are referenced to external 2,2-dimethyl-2-silapentane-5-sulfonate.

RESULTS

Absorption and CD Spectra. The absorption spectra of TmPyP4 in the presence of various stoichiometric ratios of $[d(TTAGGG)]_4$ are shown in Figure 2A. Upon the addition of $[d(TTAGGG)]_4$, the Soret band due to the porphyrin π-system exhibited a red shift from 422 to 440 nm associated

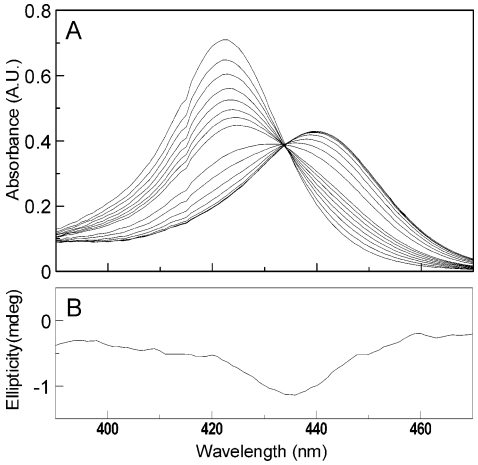

FIGURE 2: Absorption spectra of TmPyP4 in the presence of various concentrations for which $R_{TmPyP4} = 0-5.0$ (A) and CD spectrum for which $R_{TmPyP4} = 0.3$ (B) at 25 °C. [TmPyP4] = 3.0 and 6.0 μM for the absorption and CD measurements, respectively. An isosbestic point was observed at 434 nm in panel A.

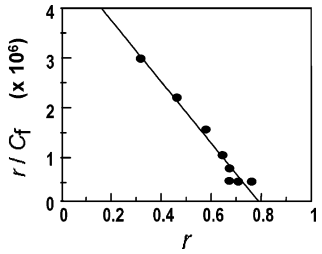

FIGURE 3: Scatchard plots of the Soret absorbance at 440 nm. The r value is the molar ratio between TmPyP4-bound $[d(TTAGGG)]_4$ and total $[d(TTAGGG)]_4$, and the concentration of the bound $[d(TTAGGG)]_4$ was determined from the analysis of the change of the 440 nm absorption. The C_f value is the concentration of free TmPyP4. The association constant and the number of binding sites were determined to be 6.2×10^6 M^{-1} and 0.79, respectively.

with 66% hypochromism, and isosbestic points were observed at 434, 498, 524, 575, 594, 629, and 645 nm. A negative CD band was induced in the Soret band by adding $[d(TTAGGG)]_4$ (Figure 2B). Furthermore, the observed isosbestic points show the presence of an equilibrium between two distinctly different environments for the porphyrin moiety of TmPyP4 in the solution mixture.

Scatchard plots of the 440 nm absorption are shown in Figure 3. The plots could be satisfactorily represented as a straight line and gave an association constant (K_a) of 6.2×10^6 M^{-1} and a number of binding sites (n) of 0.79. The stabilization energy of 38.7 kJ/mol was calculated from the obtained K_a value, 6.2×10^6 M^{-1} at 25 °C, using the relation $\Delta G = -RT \ln K_a$, where R and T are the gas constant and absolute temperature, respectively.

NMR Spectra. Downfield- and upfield-shifted portions of a 600 MHz ^{1}H NMR spectrum of $[d(TTAGGG)]_4$ at 25 °C are illustrated in trace A in Figure 4. Signal assignments were made using standard sequential assignment methods (not shown). The imino proton signals due to G4−G6 were resolved in the downfield-shifted region (10−12 ppm). Some ^{1}H NMR signals due to $[d(TTAGGG)]_4$ exhibited progressive upfield shifts and line broadening with an increasing TmPyP4 concentration ($R_{TmPyP4} = 0.0-5.0$). The differences in chemical sift changes, $\Delta\delta$ (parts per million (ppm)), of some ^{1}H NMR signals for which $R_{TmPyP4} = 1.0$ are listed in Table 1.

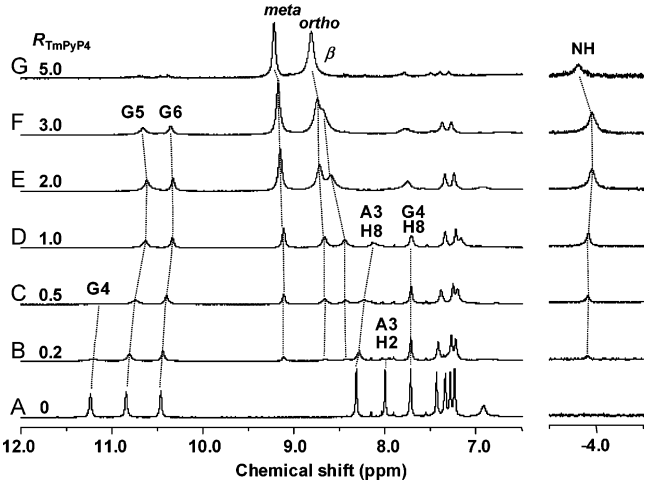

FIGURE 4: ^{1}H NMR spectra (600 MHz) of $[d(TTAGGG)]_4$ for which R_{TmPyP4} {[TmPyP4]/[$[d(TTAGGG)]_4$]} = 0 (A), 0.2 (B), 0.5 (C), 1.0 (D), 2.0 (E), 3.0 (F), and 5.0 (G) in 2 mM $[d(TTAGGG)]_4$, 50 mM potassium phosphate buffer (pH 7.0), and 300 mM KCl at 25 °C. Most DNA signals exhibited upfield shifts and were line-broadened with an increase in the R_{TmPyP4} value. The assignments of some signals are given in the spectra.

Table 1: Chemical Shifts (Δ, ppm) and Chemical Shift Changes ($\Delta\delta$, ppm) of Selected ^{1}H NMR Signals of TmPyP4 (free), $[d(TTAGGG)]_4$ (free), and a Mixture for which $R_{TmPyP4} = 1.0$ (complex) in 50 mM Potassium Phosphate Buffer (pH 7.0) and 300 mM KCl at 25 °C

	δ_{free}	$\delta_{complex}$	$\Delta\delta^a$
TmPyP4 meta	9.21	9.12	−0.09
TmPyP4 ortho	8.82	8.68	−0.14
TmPyP4 β	9.00	8.45	−0.55
TmPyP4 NH	−3.60	−3.90	−0.30
A3H8	8.32	—[b]	
A3H2	8.00	—[b]	
G4H8	7.72	7.71	−0.01
G5H8	7.43	7.34	−0.09
T1H6	7.34	—[b]	
G6H8	7.28	7.22	−0.06
T2H6	7.24	7.17	−0.07
G4 imino	11.24	—[b]	
G5 imino	10.84	10.63	−0.21
G6 imino	10.46	10.33	−0.13

[a] $\Delta\delta$ calculated as $\delta_{complex} - \delta_{free}$. [b] Could not be determined.

In particular, the A3H2, A3H8, and G4 imino proton signals exhibited significant line broadening with an increasing TmPyP4 concentration, suggesting that TmPyP4 binds to $[d(TTAGGG)]_4$ near the A3 and G4 residues and demonstrating that the time scale of formation of the complex of TmPyP4 and $[d(TTAGGG)]_4$ is faster compared with the ^{1}H NMR time scale. The observed upfield shifts of the signals for $[d(TTAGGG)]_4$ in the presence of TmPyP4 could be attributed to the ring current effect of the porphyrin moiety of TmPyP4. Further addition of TmPyP4 to $[d(TTAGGG)]_4$ resulted in considerable broadening of DNA signals. This result is partly due to an increase in the apparent molecular weight of $[d(TTAGGG)]_4$ upon complex formation with TmPyP4 and can be largely attributed to the structural inhomogeneity of the complex in the presence of a large excess of TmPyP4 relative to $[d(TTAGGG)]_4$. Therefore, in the presence of excess TmPyP4, the binding of TmPyP4 to $[d(TTAGGG)]_4$ is likely to be nonspecific. Furthermore, most TmPyP4 signals exhibited upfield shifts and line broadening in the presence of $[d(TTAGGG)]_4$.

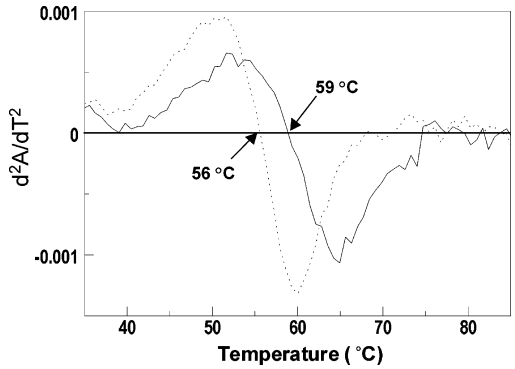

FIGURE 5: Plots of the second derivative of 260 nm absorption with respect to temperature vs temperature for R_{TmPyP4} values of 0 (···) and 1.0 (—) in 50 mM potassium phosphate buffer (pH 7.0) and 300 mM KCl. The T_m values of 56 and 59 °C were determined for R_{TmPyP4} values of 0 and 1.0, respectively.

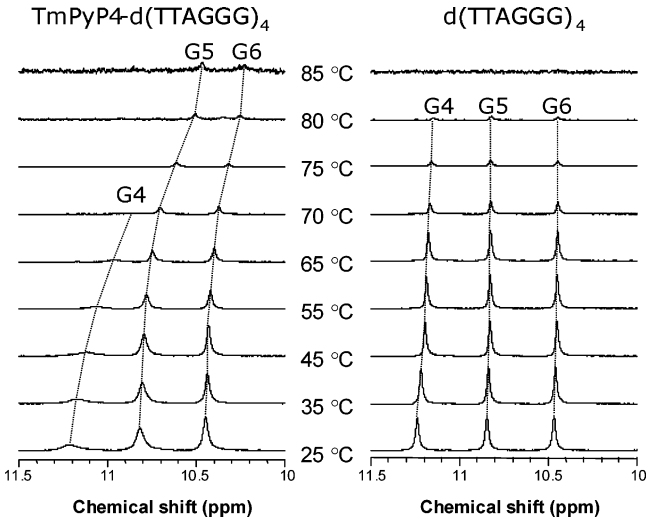

FIGURE 6: Temperature dependence of the imino proton NMR signals for R_{TmPyP4} values of 0.2 (left) and 0 (right) in 2 mM $[d(TTAGGG)]_4$, 50 mM potassium phosphate buffer (pH 7.0), and 300 mM KCl.

Effects of TmPyP4 Binding on the Stability of [d(TTAGGG)]4. The T_m values of $[d(TTAGGG)]_4$ in the absence and presence of 1.0 equivalent of TmPyP4 were determined to be 56 and 59 °C, respectively, when the temperature dependence of the 260 nm absorption is measured (Figure 5). The stability of the G-quadruplex DNA was also estimated by means of a temperature dependence study of imino proton NMR signals that were well resolved in the downfield-shifted region. Melting of the G-quadruplex DNA structure results in breaking of the hydrogen bonds, leading to the disappearance of the imino proton NMR signals in the downfield-shifted region. As shown in Figure 6, the imino proton signals of $[d(TTAGGG)]_4$ disappeared at ~80 °C, indicating dissociation of $[d(TTAGGG)]_4$ into single strands. On the other hand, in the presence of 0.2 equivalent of TmPyP4 relative to $[d(TTAGGG)]_4$, the imino proton signals could be observed up to ~85 °C. The small, but distinct, increase in the temperature at which the imino proton signals disappeared indicated that the hydrogen bonds in the G-quartets of $[d(TTAGGG)]_4$ were stabilized via binding with TmPyP4.

Observation of Intermolecular Nuclear Overhauser Effects (NOEs). The observation of intermolecular NOEs between TmPyP4 and $[d(TTAGGG)]_4$ using short mixing time reflects the interface between the molecules and hence provides direct information regarding the structure of the TmPyP4−$[d(TTAGGG)]_4$ complex. In the NOESY spectrum of a mixture for which $R_{TmPyP4} = 0.2$ recorded using a mixing time of 200 ms (Figure 7), the meta proton signal of TmPyP4 exhibited NOE connectivities with the G4H1′, G4H4′, A3H1′, A3H4′, and T2H4′ protons and the ortho proton and the β-protons of TMPyP4 with the A3H2 and A3H8 protons. Thus, the DNA protons exhibiting intermolecular NOEs with TmPyP4 protons are mostly located near the A3pG4 step region (Figure 8).

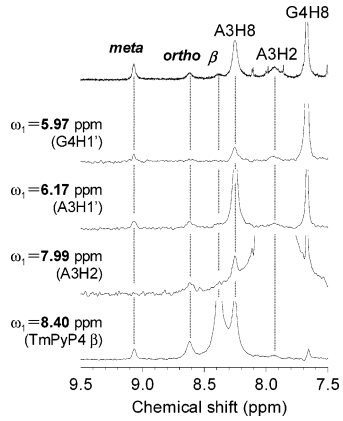

FIGURE 7: Slices of the NOESY spectrum of a mixture for which $R_{TmPyP4} = 0.2$ at 25 °C, recorded using a mixing time of 200 ms. The signal assignments are shown in the spectra.

DISCUSSION

Binding of TmPyP4 to [d(TTAGGG)]4. The high sensitivity of the Soret band to the chemical environment of the porphyrin ring allowed not only thermodynamic characterization of the binding of TmPyP4 to DNAs but also characterization of the intermolecular association between them (*31*). Both intercalation and groove binding have been reported for formation of the complexes of TmPyP4 with DNAs. The intercalation of TmPyP4 into CG pairs of duplex DNA has been shown to result in a red shift of ~20 nm for the Soret absorption, together with a large hypochromicity (~50%) of the band and a negative induced-CD band (*16*). On the other hand, the groove binding of TmPyP4 to AT pairs of duplex DNA usually results in a small red shift (~10 nm), together with a small hypochromicity (~20%) and a positive induced-CD band (*16*). Furthermore, the binding of TmPyP4 to antiparallel G-quadruplex DNA exhibited a red shift of ~20 nm and large hypochromicity for the Soret band, associated with a negative induced-CD band (*26*). In the system described here, the Soret absorption and CD changes, i.e., a 18 nm red shift of the band with 66% hypochromicity and a negative induced-CD band, observed for TmPyP4 upon addition of $[d(TTAGGG)]_4$ were consistent with the intercalation of TmPyP4 into G-quadruplex DNA (*26*, *27*, *29*).

The K_a value (6.2×10^6 M^{-1}) obtained for the TmPyP4−$[d(TTAGGG)]_4$ complex was within the range of K_a values (10^4−10^6 M^{-1}) reported for the binding of TmPyP4 to G-quadruplex DNA (*29*) and was slightly higher than the apparent K_a value (2.3×10^5 M^{-1}) observed for the intercalation of TmPyP4 into poly(G-C) in the presence of 315 mM Na^+ (*36*). Since $[d(TTAGGG)]_4$ forms a dimer in

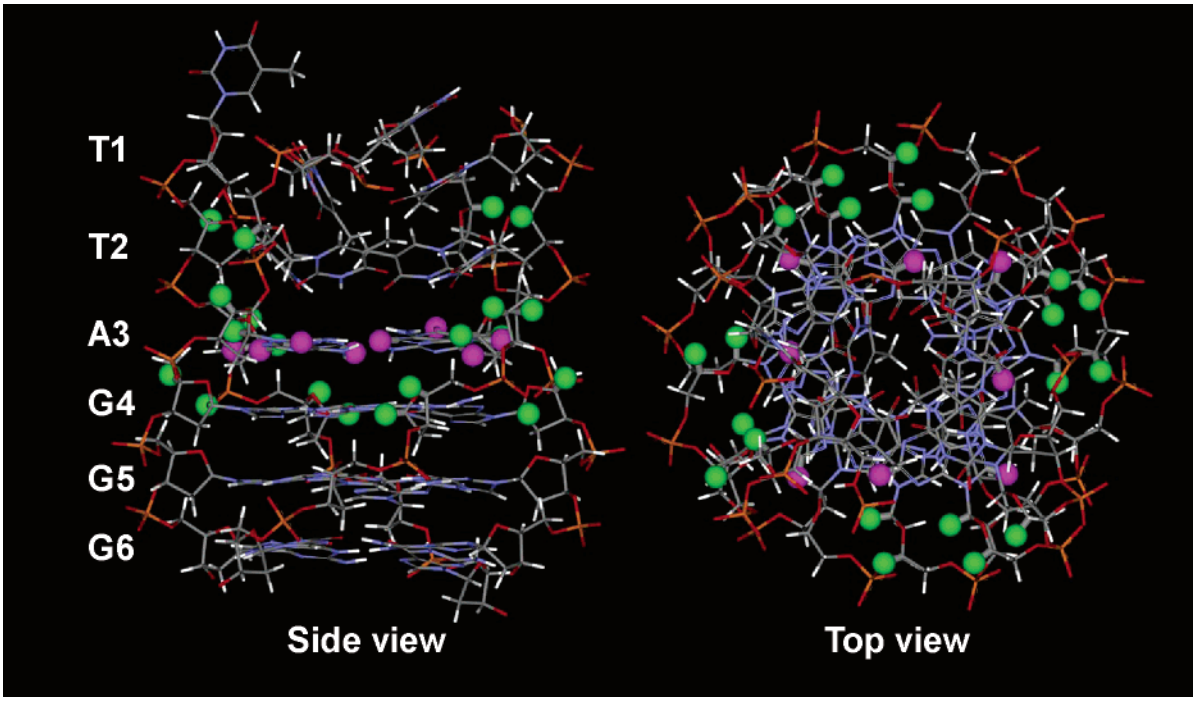

FIGURE 8: Protons of $[d(TTAGGG)]_4$ that exhibited NOE connectivities with ortho protons and β-protons (pink) and the meta proton (green) of TmPyP4. The structure of $[d(TTAGGG)]_4$ is taken from the NMR structure of $[d(TTAGGGT)]_4$ (PDB entry 1NP9) (*48*).

solution through intermolecular end-to-end stacking of the G-quartets formed by G6 guanine bases (*44*), the interface between the G-quartets formed by G6 guanine bases in the $[d(TTAGGG)]_4$ dimer could be a potential binding site for TmPyP4, leading to a 1:2 stoichiometry for the complex formation, i.e., an *n* value of 0.5. But the obtained *n* value of 0.79 can be approximated to 1, i.e., a 1:1 stoichiometry for formation of the complex of TmPyP4 and $[d(TTAGGG)]_4$. In fact, the NMR results supported the fact that TmPyP4 intercalates into the A3pG4 step of $[d(TTAGGG)]_4$ (see below).

Structure of the TmPyP4−[d(TTAGGG)]$_4$ Complex. Intermolecular NOE connectivities useful for the structural characterization of the TmPyP4−$[d(TTAGGG)]_4$ complex can be observed, as illustrated in Figures 7 and 8. For example, the sugar ring H1′ protons of A3 and G4 and the H4′ protons of T2, A3, and G4 exhibited NOEs to a meta proton that occupies the position farthest from the center of mass for TmPyP4. Furthermore, the H2 and H8 protons of the A3 base exhibited NOEs to the ortho proton and β-protons of TmPyP4. These results suggested that TmPyP4 is accommodated near the A3pG4 step. Additionally, NMR signals due to the H2 and H8 protons of the A3 base and the imino proton of G4 were greatly affected by formation of the complex with TmPyP4, also supporting the specific binding of TmPyP4 between the A3 and G4 residues in $[d(TTAGGG)]_4$.

The TmPyP4 meta, ortho, and β-proton signals exhibited upfield shifts upon formation of the complex with the G-quadruplex (Table 1). These protons are ranked as follows in order of increasing magnitude of the induced shift change: meta < ortho < β. Thus, the shift induced upon formation of the complex with DNA is smaller for protons farther from the center of mass for TmPyP4, supporting the interaction of the porphyrin moiety of TmPyP4 with G-quadruplex DNA. These results supported the occurrence of $\pi-\pi$ stacking between the TmPyP4 porphyrin moiety and the G-quartet in the TmPyP4−$[d(TTAGGG)]_4$ complex.

The imino proton signals of G4−G6 of $[d(TTAGGG)]_4$ exhibited progressive upfield shifts and line broadening with an increase in the R_{TmPyP4} value. The upfield shifts of these imino proton signals can be attributed predominantly to the ring current effect of the porphyrin ring of TmPyP4. Assuming that the maximum interaction between the π-systems of the porphyrin moiety of TmPyP4 and the G-quartet formed from G4 bases of the quadruplex DNA in the TmPyP4−$[d(TTAGGG)]_4$ complex, the TmPyP4 porphyrin plane is located ~0.35, ~0.70, and ~1.05 nm from the planes of the G-quartets formed from G4, G5, and G6 bases, respectively, of the quadruplex DNA (see the Supporting Information), and according to the reported equation for the ring current effects of a porphyrin (*45*), the upfield shifts of ~3.36, ~1.10, and ~0.40 ppm were expected for the imino proton signals of G4, G5, and G6, respectively, due to the TmPyP4 porphyrin ring current. Furthermore, a displacement of the TmPyP4 porphyrin ring relative to the DNA leads to a removal of the equivalence for all four imino protons of each G-quartet. Thus, the G4 imino proton signal is most sensitive to the orientation of the TmPyP4 porphyrin ring. Consequently, the observation of the largest TmPyP4-induced line broadening for the G4 imino proton signal may be interpreted in terms of internal dynamics of TmPyP4 within the TmPyP4−$[d(TTAGGG)]_4$ complex, in addition to the dynamics of the complex formation reaction. In fact, as shown in Figure 6, the imino proton signals of the TmPyP4−$[d(TTAGGG)]_4$ complex at ambient temperature are ranked as G6 < G5 < G4, in order of increasing the line width, supporting the contribution of the internal dynamics of TmPyP4 in the complex to the line width of the imino proton signals.

Model Study of the TmPyP4−[d(TTAGGG)]$_4$ Complex. For the TmPyP4−$[d(TTAGGG)]_4$ complex, the observed

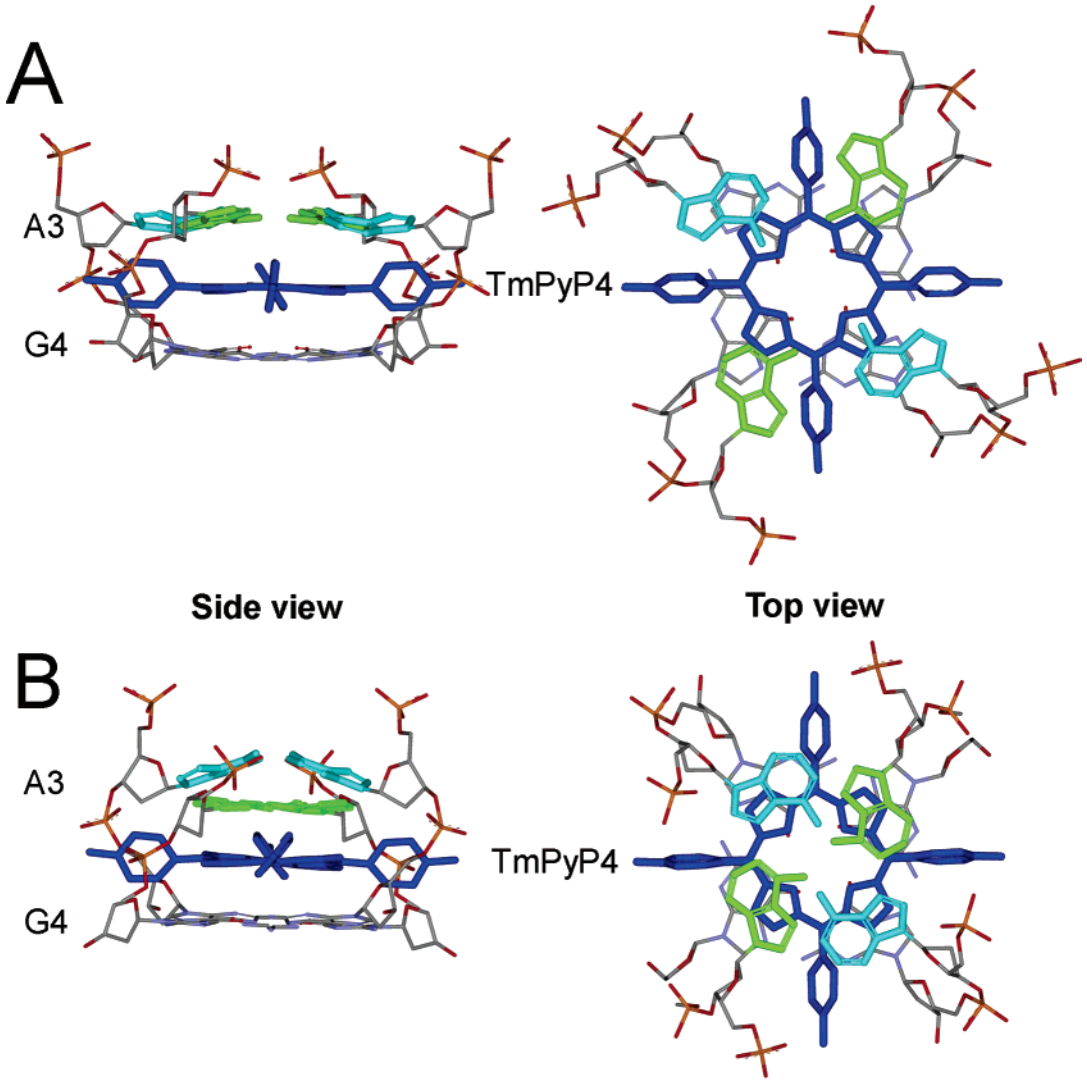

FIGURE 9: Plausible models of intercalation of TmPyP4 into the A3pG4 step proposed from the molecular mechanics calculation. The optimum structure of TmPyP4 determined by PM3 calculation (see the Supporting Information) was placed in the middle of the A3pG4 step which was taken from the NMR structure of $[d(TTAGGGT)]_4$ (PDB entry 1NP9) (*48*). One of the optimum structures, obtained from the molecular mechanics calculation using the MM2 force field on Chem3D (*46*), is illustrated in panel A. The structure obtained from a similar calculation, with the displacement of two A3 adenine bases facing each other ~0.3 nm above the A3 quartet plane, is illustrated in panel B. The A3pG4 portion of $[d(TTAGGG)]_4$ is illustrated in CPK color, the exception being the pairs of A3 adenine bases facing each other illustrated in green and cyan and TmPyP4 in blue.

intermolecular NOEs were centered at the A3pG4 step (Figure 8). The NOEs between TmPyP4 and the A3 base demonstrated a stacking interaction between the porphyrin moiety of TmPyP4 and the A3 adenine base. We constructed two plausible models for intercalation of TmPyP4 into the A3pG4 step using the molecular mechanics calculation (*46*) (Figure 9 and the Supporting Information). In the models, all four or only two A3 adenine bases can stack onto the porphyrin moiety of TmPyP4 without a large conformation change of the G-quadruplex DNA. In both cases, the intercalation of TmPyP4 into the A3pG4 step of the G-quadruplex DNA can be stabilized by sandwiching the TmPyP4 porphyrin moiety with the A3 adenine bases and the G4 quartet. Furthermore, the electrostatic interaction between the *N*-methylpyridinium ions of TmPyP4 and phosphate ions of the DNA also contributes to the stabilization of the TmPyP4−$[d(TTAGGG)]_4$ complex. As illustrated in Figure 9, *N*-methylpyridinium side chains of TmPyP4 are likely to be accommodated between the DNA backbones in the TmPyP4−$[d(TTAGGG)]_4$ complex, and hence, the pyridinium cations partially neutralize the nearby DNA phosphate anions, stabilizing the complex through the electrostatic interaction. The orientation of four *N*-methylpyridinium ions of TmPyP4 is well-suited for electrostatic interaction with phosphate ions of G-quadruplex DNA (Figure 10).

A study of formation of the complex of TmPyP4 with antiparallel and parallel G-quadruplex DNAs formed from a series of DNA sequences indicated that TmPyP4 intercalates between G-quartets with an association constant of 10^4−10^6 M^{-1} (*27*, *29*, *47*). On the other hand, this study demonstrates that TmPyP4 does not intercalate between the G-quartets of $[d(TTAGGG)]_4$ but preferentially binds to the A3pG4 step with an association constant of 6.2×10^6 M^{-1}. Due to steric hindrance between the ortho proton of the *N*-methylpyridinium group and the β-proton of the pyrrole ring in TmPyP4, the pyridinium and porphyrin planes cannot be coplanar with each other (see the Supporting Information).

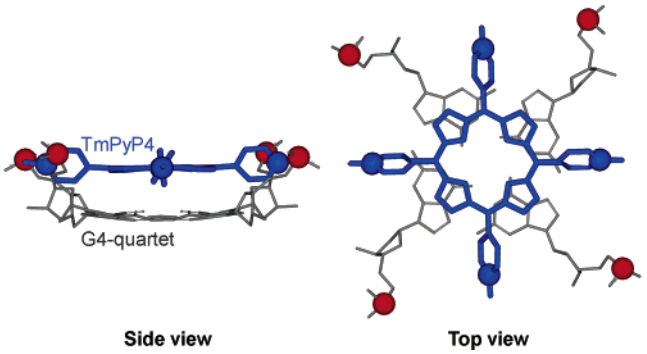

FIGURE 10: Orientation of *N*-methylpyridinium ions (blue) of TmPyP4 with respect to phosphate ions (red) of the G4 quartet. Blue and gray lines represent TmPyP4 and G4 quartet, respectively. The distance between the pyridinium ion and phosphate ion is ~0.8 nm.

Such a restraint of TmPyP4 conformation causes unfavorable steric hindrance upon its intercalation into the GpG step, and in fact, the distance between adjacent G-quartets needs to be increased for the accommodation of TmPyP4. Therefore, the association constant for binding of TmPyP4 to the GpG step is smaller by more than 1 order of magnitude compared with that for binding to the ApG step (*27*). Thus, stacking interaction between the π-systems of TmPyP4 and DNA bases plays a significant role in determining the stability of the TmPyP4−[d(TTAGGG)]$_4$ complex as well as the molecular recognition between them. The relatively flexible 5′-terminal TTA region of [d(TTAGGG)]$_4$ could be suitable for the accommodation of TmPyP4 at the A3pG4 step because the porphyrin ring of TmPyP4 can be sandwiched between the G4 quartet and A3 bases. These findings provide novel insights into the molecular recognition between porphyrin derivatives and DNA.

ACKNOWLEDGMENT

We thank Professor Toshiyuki Tanaka (Institute of Applied Biochemistry, University of Tsukuba) for the valuable suggestions. The NMR spectra were recorded on Bruker AVANCE-500 and -600 spectrometers at the Chemical Analysis Center, University of Tsukuba.

SUPPORTING INFORMATION AVAILABLE

Determination of K_a and n (SI-1), determination of stabilization energies (SI-2), ring current effect of TmPyP4 porphyrin on the G4−G6 imino proton shifts (SI-3), an energy-optimized structure of TmPyP4 (SI-4), and plausible models of TmPyP4−[d(TTAGGG)]$_4$ complex (SI-5 and SI-6). This material is available free of charge via the Internet at http://pubs.acs.org.

REFERENCES

1. Wang, Y., and Patel, D. J. (1993) Solution structure of a parallel-stranded G-quadruplex, DNA, *J. Mol. Biol. 234*, 1171−1183.
2. Wang, Y., and Patel, D. J. (1993) Solution structure of the human telomeric repeat d[AG3(T2AG3)3] G-tetraplex, *Structure 15*, 263−282.
3. Haider, S., Parkinson, G. N., and Neidle, S. (2002) Crystal structure of the potassium form of an *Oxytricha nova* G-quadruplex, *J. Mol. Biol. 320*, 189−200.
4. Parkinson, G. N., Lee, M. P. J., and Neidle, S. (2002) Crystal structure of parallel quadruplexes from human telomeric DNA, *Nature 417*, 876−880.
5. Li, J., Correia, J. J., Wang, L., Trent, J. O., and Chaires, J. B. (2005) Not so crystal clear: The structure of the human telomere G-quadruplex in solution differs from that present in a crystal, *Nucleic Acid Res. 33*, 4649−4659.
6. Blasco, M. A. (2005) Telomeres and human disease: Aging, cancer and beyond, *Nat. Rev. Genet. 6*, 611−622.
7. Mergny, J.-J., and Hélène, C. (1998) G-Quadruplex DNA: A target for drug design, *Nat. Med. 4*, 1366−1367.
8. Han, H., and Hurley, L. H. (2000) G-Quadruplex DNA: A potential target in anticancer drug design, *Trends Pharmacol. Sci. 21*, 136−142.
9. Hurley, L. H., Wheelhouse, R. T., Sun, D., Kerwin, S. M., Salazar, M., Fedoroff, O. Y., Han, F. X., Izbicka, E., and von Hoff, D. D. (2000) G-Quadruplexes as targets for drug design, *Pharmacol. Ther. 85*, 141−158.
10. Kerwin, S. (2000) G-quadruplex DNA as a target for drug design, *Curr. Pharm. Des. 6*, 441−471.
11. Fiel, R. J. (1989) Porphyrin-nucleic acid interactions: A review, *J. Biomol. Struct. Dyn. 6*, 1259−1274.
12. Verlhac, J. B., and Gaudemer, A. (1984) Water-soluble porphyrins and metalloporphyrins as photosensitizers in aerated aqueous solutions. I. Detection and determination of quantum yield of formation of singlet oxygen, *Nouv. J. Chim. 8*, 401−406.
13. Villanueava, A., Juarranz, A., Diaz, V., Gomez, J., and Canete, M. (1992) Photodynamic effects of a cationic mesosubstituted porphyrin in cell culture, *Anti-Cancer Drug Des. 7*, 297−303.
14. Izbicka, E., Nishioka, D., Marcell, V., Raymond, E., Davidson, K. K., Lawrence, R. A., Wheelhouse, R. T., Hurley, L. H., Wu, R. S., and von Hoff, D. D. (1999) Telomere-interactive agents affect proliferation rates and induce chromosomal destabilization in sea urchin embryos, *Anti-Cancer Drug Des. 14*, 355−365.
15. Rha, S. Y., Izbicka, E., Lawrence, R., Davidson, K., Sen, D., Moyer, M. P., Roodman, G. D., Hurley, L. H., and von Hoff, D. D. (2000) Effect of telomere and telomerase interactive agents on human tumor and normal cell lines, *Clin. Cancer Res. 6*, 987−993.
16. Pasternack, R. F. (1986) The influence of ionic strength on the binding of a water soluble porphyrin to nucleic acids, *Nucleic Acids Res. 14*, 5919−5931.
17. Ford, K. G., and Neidle, S. (1995) Perturbation in DNA structure upon interaction with porphyrin revealed by chemical probes, DNA footprinting and molecular modeling, *Bioorg. Med. Chem. 3*, 671−677.
18. Gandini, S. C. M., Borissevitch, L. E., Perussi, J. R., Imasato, H., and Tabak, M. (1998) Aggregation of *meso*-tetrakis(4-*N*-methylpyridiniumyl) porphyrin in its free base, Fe(III) and Mn(III) forms due to the interaction with DNA in aqueous solutions: Optical absorption, fluorescence and light scattering studies, *J. Lumin. 78*, 53−61.
19. Wheelhouse, R. T., Sen, D., Han, H., Han, F. X., and Hurley, L. H. (1998) Cationic porphyrins as telomerase inhibitors: The interaction of tetra-(*N*-methyl-4-pyridyl)porphine with quadruplex DNA, *J. Am. Chem. Soc. 120*, 3261−3262.
20. Guliaev, A. B., and Leontis, N. B. (1999) Cationic 5,10,15,20-tetrakis(*N*-methylpyridinium-4-yl)porphyrin fully intercalates at 5′-CG-3′ step of duplex DNA solution, *Biochemistry 38*, 15425−15437.
21. Lee, S., Lee, Y. A., Lee, H. M., Lee, J. Y., Kim, D. H., and Kim, S. K. (2002) Rotation of periphery methylpyridine of *meso*-tetrakis(*n*-*N*-methylpyridiniumyl)porphyrin (n = 2, 3, 4) and its selective binding to native and synthetic DNAs, *Biophys. J. 83*, 371−381.
22. Lee, Y. A., Lee, S., Cho, T. S., Han, S. W., and Kim, S. K. (2002) Binding mode of *meso*-tetrakis(*N*-methylpyridinium-4-yl)porphyrin to poly[d(I-C)$_2$]: Effect of amino groups at the minor groove of poly[d(G-C)$_2$] on the porphyrin-DNA interaction, *J. Phys. Chem. B 106*, 11351−11355.
23. Uno, T., Hamasaki, K., Taniguchi, M., and Shimabayashi, S. (1997) Binding of *meso*-tetrakis(*N*-methylpyridinium-4-yl)porphyrin to double helical RNA and DNA·RNA hybrids, *Inorg. Chem. 36*, 1676−1683.
24. Ren, J., and Chaires, J. B. (1999) Sequence and structural selectivity of nucleic acid-binding ligands, *Biochemistry 38*, 16067−16075.
25. Lee, Y. A., Kim, J., Cho, T., Song, R., and Kim, S. K. (2003) Binding of *meso*-tetrakis(*N*-methylpyridium-4-yl)porphyrin to triplex oligonucleotides: Evidence for porphyrin stacking in the major groove, *J. Am. Chem. Soc. 125*, 8106−8107.

26. Anantha, N. V., Azam, M., and Sheardy, R. D. (1998) Porphyrin binds to quadruplexed T_4G_4, *Biochemistry 37,* 2709−2714.
27. Haq, I., Trent, J. O., Chowdhry, B. Z., and Jenkins, T. C. (1999) Interactive G-tetraplex stabilization of telomeric DNA by a cationic porphyrin, *J. Am. Chem. Soc. 121,* 1768−1779.
28. Fedoroff, O. Y., Rangan, A., Chemeris, V. V., and Hurley, L. H. (2000) Cationic porphyrin promote the formation of i-motif DNA and bind peripherally by a nonintercalative mechanism, *Biochemistry 39,* 15083−15090.
29. Han, H., Langley, D. R., Rangan, A., and Hurley, L. H. (2001) Selective interaction of cationic porphyrin with G-tetraplex structures, *J. Am. Chem. Soc. 123,* 8902−8913.
30. Shi, D., Wheelhouse, R. T., Sen, D., and Hurley, L. H. (2001) Quadruplex-interactive agents as telomerase inhibitors: Synthesis of porphyrin and structure−activity relationship for the inhibition of telomerase, *J. Med. Chem. 44,* 4509−4523.
31. Pasternack, R. F., Gibbs, E. J., and Villafranca, J. J. (1983) Interaction of porphyrins with nucleic acids, *Biochemistry 22,* 2406−2414.
32. Marzilli, L. G., Banville, D. L., and Zon, G. (1986) Pronounced ^{1}H and ^{31}P NMR spectral changes on *meso*-tetrakis(*N*-methylpyridinium-4-yl)porphyrin binding to teradecaoligo-deoxyribonucleotides: Evidence for symmetric, selective binding to 5′CG3′ sequences, *J. Am. Chem. Soc. 108,* 4188−4192.
33. Ohyama, T., Mita, H., and Yamamoto, Y. (2005) Binding of 5,10,15,20-tetrakis(*N*-methylpyridinium-4-yl)-21*H*,23*H*-porphyrin to an AT-rich region of a duplex DNA, *Biophys. Chem. 113,* 53−59.
34. Kim, J., Lee, Y., Yun, B. H., Han, S. W., Kwag, S. T., and Kim, S. K. (2004) Binding of meso-tetrakis(*N*-methylpyridinium-4-yl)-porphyrin to AT oligomers: Effect of chain length and the location of the porphyrin stacking, *Biophys. J. 86,* 1012−1017.
35. Lee, S., Jeon, S. H., Kim, B. J., Han, S. W., Jang, H. G., and Kim, S. K. (2001) Classification of CD and absorption spectra in the Soret band of H_2TMPyP bound to various synthetic polynucleotides, *Biophys. Chem. 92,* 35−45.
36. Strickland, J. A., Marzilli, L. G., Gay, K. M., and Wilson, W. D. (1988) Porphyrin and metalloporphyrin binding to DNA polymers: Rate and equilibrium binding studies, *Biochemistry 27,* 8870−8878.
37. Sriram, M., van der Marel, G. A., Roelen, H. L. P. F., van Boom, J. H., and Wang, A. H. J. (1992) Structural consequences of a carcinogenic alkylation lesion on DNA: Effect of O6-ethylguanine [e6G] on the molecular structure of the d(CGC[e6G]AATTCGCG)-netropsin complex, *Biochemistry 31,* 11823−11834.
38. Ellervik, U., Wang, C. C. C., and Dervan, P. B. (2000) Hydroxybenzamide/pyrrole pair distinguishes T·A from A·T base pairs in the minor groove of DNA, *J. Am. Chem. Soc. 122,* 9354−9360.
39. Lah, J., and Vesnaver, G. (2000) Binding of distamycin A and netropsin to 12mer DNA duplexes containing mixed AT·GC sequences with at most five or three successive AT base pairs, *Biochemistry 39,* 9317−9326.
40. Wang, Y., and Patel, D. J. (1992) Guanine residues in d(T_2AG_3) and d(T_2G_4) form parallel-stranded potassium cation stabilized G-tetraplexes with anti glycosidic torsion angles in solution, *Biochemistry 31,* 8112−8119.
41. Pitto, M., Saudek, V., and Sklenar, V. (1992) Gradient-tailored excitation for single-quantum NMR spectroscopy of aqueous solutions, *J. Biomol. NMR 2,* 661−666.
42. Sklenar, V., Pitto, M., Leppik, R., and Saudek, V. (1993) Gradient-tailed water suppression for ^{1}H-^{15}N HSQC experiments optimized to retain full sensitivity, *J. Magn. Reson., Ser. A 102,* 241−245.
43. States, D. J., Haeberkorn, R. A., and Ruben, D. J. (1982) A two-dimensional nuclear Overhauser experiment with pure absorption phase in four quadrants, *J. Magn. Reson. 72,* 286−292.
44. Kato, Y., Ohyama, T., Mita, H., and Yamamoto, Y. (2005) Dynamics and thermodynamics of dimerization of parallel G-tetraplexed DNA formed from d($TTAG_n$) ($n = 3-5$), *J. Am. Chem. Soc. 127,* 9980−9981.
45. Abraham, R. J., and Medforth, C. J. (1988) The NMR spectra of the porphyrins, *Magn. Reson. Chem. 26,* 803−812.
46. Burkart, U., and Allinger, N. L. (1982) Molecular mechanics, in *Computational Chemistry* (Clark, T., Ed.) Wiley, New York.
47. Kim, M. Y., Gleason-Guzman, M., Izbicka, E., Nishioka, D., and Hurley, H. L. (2003) The different biological effect of telomestatin and TMPyP can be attributed to their selectivity for interaction with intramolecular or intermolecular G-quadruplex structure, *Cancer Res. 63,* 3247−3256.
48. Gavathiotis, E., and Searle, M. S. (2003) Structure of the parallel-stranded DNA quadruplex d($TTAGGGT)_4$ containing the human telomeric repeat: Evidence for A-tetrad formation from NMR and molecular dynamics simulations, *Org. Biomol. Chem. 1,* 1650−1656.

BI052442Z